Polarization-Driven Topological Insulator Transition in a GaN/InN/GaN Quantum Well

M. S. Miao,[1,3,*] Q. Yan,[1] C. G. Van de Walle,[1] W. K. Lou,[2] L. L. Li,[2] and K. Chang[2,3,†]

[1]Materials Research Laboratory and Materials Department, University of California, Santa Barbara, California 93106-5050, USA
[2]SKLSM, Institute of Semiconductors, Chinese Academy of Sciences, P.O. Box 912, Beijing 100083, People's Republic of China
[3]Beijing Computational Science Research Center, Beijing 10084, People's Republic of China

(Received 8 May 2012; published 2 November 2012)

Topological insulator (TI) states have been demonstrated in materials with a narrow gap and large spin-orbit interactions (SOI). Here we demonstrate that nanoscale engineering can also give rise to a TI state, even in conventional semiconductors with a sizable gap and small SOI. Based on advanced first-principles calculations combined with an effective low-energy $\mathbf{k} \cdot \mathbf{p}$ Hamiltonian, we show that the intrinsic polarization of materials can be utilized to simultaneously reduce the energy gap and enhance the SOI, driving the system to a TI state. The proposed system consists of ultrathin InN layers embedded into GaN, a layer structure that is experimentally achievable.

DOI: 10.1103/PhysRevLett.109.186803 PACS numbers: 72.25.Dc, 73.21.Cd, 75.70.Tj, 77.22.Ej

Topological insulators (TIs), a new state of quantum matter, have recently attracted significant attention, both for their fundamental research interest and for their potential device applications [1–3]. The TI state can be achieved in semiconductors with inverted bands [Fig. 1(a)] and is usually driven by the intrinsic spin-orbit interaction (SOI) arising from heavy host atoms [4,5]. In the TI state the system features an insulating bulk and gapless surface or edge states. These novel states show a linear Dirac spectrum that is protected by time-reversal symmetry, resulting in quantized and robust conductance when the Fermi level is in the gap.

This new quantum state of electrons was first proposed theoretically for quantum wells (QWs) and then for three-dimensional cases, and was later demonstrated experimentally by angle-resolved photoemission spectroscopy [6,7]. Early efforts to find TI materials focused on binary II-VI compounds or chalcogenides with heavy atoms, such as HgTe and Bi_2X_3 ($X = $ Te, Se) [7]. By adjusting the thickness or strain of a CdTe/HgTe/CdTe QW, or applying an external electric field, one can drive the system into the TI phase. The investigations have been extended to ternary Heusler compounds, with first-principles calculations playing an important role [8–10].

In spite of such progress, the search for TIs in more commonly used semiconductor systems has remained elusive, holding out the prospect of integration with conventional semiconductor devices. However, commonly used semiconductors typically have sizable band gaps and insignificant SOI, in contrast to the requirements for a TI phase transition. One promising approach is to apply a strong gate voltage in a two-dimensional nanoscale QW system [11,12]. The strong electric field reduces the gap and induces considerable Rashba SOI that may transform the system into a TI. The major difficulty of this approach is that the required electric field is very strong and typically reduces the gap by less than 0.1 eV.

Here we propose that the intrinsic polarization of materials can be utilized to reduce the energy gap and invert the band ordering at the Γ point. The wurtzite structure of the III-nitrides allows for the presence of spontaneous and piezoelectric polarization fields in structures grown along the [0001] direction. The piezoelectric fields arise due to the large strain that is induced in a thin InN layer grown pseudomorphic ally on GaN (i.e., maintaining the in-plane lattice constant of the GaN layer; we assume growth on a GaN substrate or thick GaN layer). We show by first-principles electronic structure calculations that this

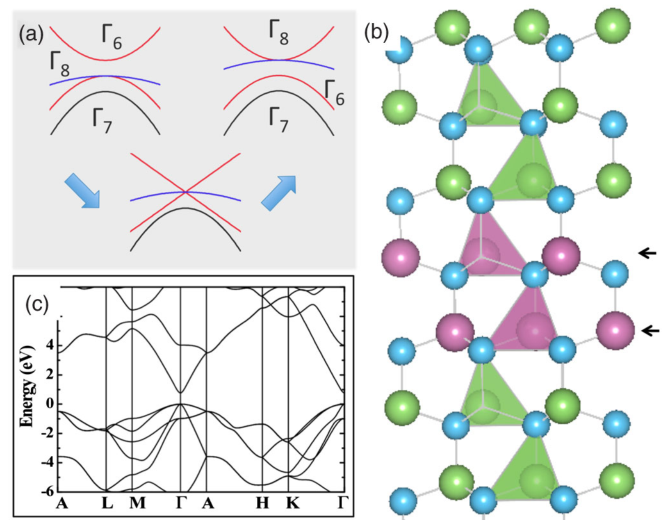

FIG. 1 (color online). (a) Counterclockwise, bands of normal semiconductors such as CdTe, bands at the zero-gap transition point, and inverted bands of semiconductors. (b) Side view of a GaN/InN/GaN QW including two atomic layers of InN in a GaN matrix along the (0001) polar orientation. Small blue balls represent N atoms, purple balls In, and blue balls Ga; the In atomic layers are marked by arrows. (c) Calculated band structure of bulk InN using the HSE hybrid functional.

 © 2012 American Physical Society

polarization can invert the bands of a GaN/InN/GaN QW when the InN thickness exceeds three monolayers (ML)–a ML being defined as a double layer of In and N (with a thickness of 3.12 Å in strained InN) along the [0001] axis. We then use an eight-band $\mathbf{k} \cdot \mathbf{p}$ model that includes both SOI and the strong polarization field to prove that such a system can become a TI and possess edge states in the energy gap of a Hall bar structure.

The proposed TI has many unique advantages, including (1) it can be realized based on commonly used semiconductors and be integrated into various devices, (2) it is driven by large intrinsic polarization fields, (3) the TI state can be manipulated by applying external fields or injecting charge carriers and can be adjusted by standard semiconductor techniques, including doping, alloying and varying the QW thickness, and (4) the polarization field can induce a large Rashba SOI in this system containing only light elements, which provides a new approach to manipulating spin freedom in such systems.

Our proposed QW consists of InN layers sandwiched between GaN along the [0001] direction [Fig. 1(b)]. Group-III nitrides (III-N), including InN, GaN, and AlN, have been intensively studied because of their applications in light emitters, high-frequency transistors, and many other areas. An important feature of III-N compounds is that although their band gap varies from 0.7 eV to 6.2 eV, all three compounds and their alloys are stable in the same wurtzite structure with relatively modest variations in a lattice constant. This feature, combined with advanced growth techniques, allows the fabrication of high-quality alloys and heterojunctions. InN has a fundamental gap of only ~0.7 eV [13], resulting in strong coupling between the electron and hole states and leading to a large nonparabolicity of the bands around the Γ point [Fig. 1(c)] as well as an exceedingly small electron effective mass of $0.067m_0$ [14].

Our first-principles calculations are based on density functional theory (DFT) with a plane-wave basis set and projector augmented waves [15], as implemented in the VASP program [16]. Because the accuracy of the band gap is of key importance for this Letter, we employ a hybrid functional [17]. Recent calculations have demonstrated the reliability of this approach for producing structural parameters as well as band gaps in agreement with experiment. Using a standard mixing parameter of 0.25, we found the band gaps of GaN and InN to be 3.25 and 0.62 eV (Ref. [18]). The lattice parameters $a = b$ and c are found to be 3.182 and 5.175 Å for GaN and 3.548 and 5.751 Å for InN. The GaN/InN/GaN QW is modeled by a supercell consisting of 1 to 5 atomic layers of InN and 23 or 24 atomic layers of GaN (periodicity requires that the total number of atomic layers be even). The SOI is not included in the first-principles calculations, but its effect is included in the $\mathbf{k} \cdot \mathbf{p}$ model.

Figures 2(a) and 2(b) show band structures around the Γ point calculated with DFT using the hybrid functional of Heyd, Scuseria and Ernzerhof (HSE) [17], and Fig. 2(c) shows the band gap as a function of the number of InN layers. At 2 ML, the system has a gap of 0.82 eV (larger than the fundamental gap due to strain and quantum confinement), but at 3 ML this is reduced to 0.06 eV [Fig. 2(c)]. In both these cases, the band structures are still normal in the sense that the heavy hole (HH) and light hole (LH) states are degenerate at the Γ point (Γ_6) and are lower in energy than the electron state (E) (Γ_1). At 4 ML, however, the system exhibits an inverted band structure, in which the Γ_6 states are 0.10 eV higher than the Γ_1 state. In Figs. 2(a) and 2(b), the states around the Γ point are denoted by their symmetry. Such an inverted band structure is a signature of the transition to a TI state.

We now discuss the details of this transition to an inverted band structure. For an ultra-thin QW, the gap between the valence and conduction states is determined by the interplay of three factors, namely quantum confinement, polarization field, and strain. The quantum-confinement effect is large for these thin QWs, explaining

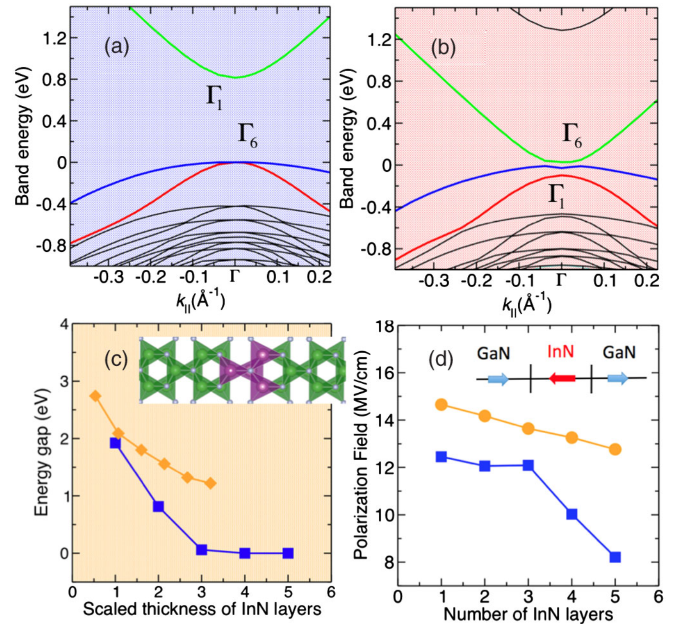

FIG. 2 (color online). (a) and (b) Band structure of a GaN/InN/GaN QW around the Γ point for 2 and 4 ML of InN, based on first-principles DFT-HSE calculations. The green lines represent electron states, red lines light-hole states, and blue lines heavy-hole states. (c) Calculated energy gaps as a function of the thickness of InN layers for polar ([0001]) (blue squares) and nonpolar ([10$\bar{1}$0]) (orange diamonds) GaN/InN/GaN QWs. The thicknesses were scaled to the thickness of 1 ML of InN in a polar QW and therefore correspond to the number of InN layers in the polar case. The inset shows a [10$\bar{1}$0] QW with two InN layers. (d) Polarization field as a function of number of inserted InN layers calculated by DFT-HSE (blue squares) and based on theoretical polarization constants (orange circles). The blue and red block arrows in the inset show the polarization direction of GaN and InN regions [19].

why the 1 ML and 2 ML QWs have gaps larger than bulk InN. However, the effect on the band gap becomes smaller than 0.1 eV when the thickness of the InN QW exceeds 3 ML.

The effect of polarization, on the other hand, increases with increasing QW thickness. The difference in spontaneous polarization between InN and GaN, along with the piezoelectric polarization induced by the strain in InN, generates polarization charges [Fig. 2(d)] that give rise to an electric field in the InN layer. (Depending on the details of the structure and the boundary conditions, electric fields may also be present in the surrounding GaN layers.) This polarization field leads to a potential drop over the InN QW, and localizes hole states and electron states on opposite sides of the QW. As the QW width increases the electron and hole states become closer in energy, leading to a significant reduction in overall band gap [Fig. 2(c)].

In order to demonstrate that the band inversion is driven by the polarization fields we also performed calculations for GaN/InN/GaN QWs in a nonpolar ($[10\bar{1}0]$) orientation. Quantum-confinement effects and strains are similar for the two orientations, so the enhanced reduction in band gap for the polar QW observed in Fig. 2(c) can be attributed to the presence of polarization fields. In contrast, the gap for the nonpolar QW saturates to a value around 1 eV (different from the bulk gap due to the presence of compressive strain in the InN layer).

The electric field in the InN layers [Fig. 2(d)] is as large as 12.5 MV/cm. This field is in principle due to strain-induced piezoelectric polarization as well as spontaneous polarization. Because the spontaneous polarization constants of GaN and InN are quite similar, and because the strains are very large in these pseudomorphic layers, the piezoelectric field dominates.

The first-principles results included in Fig. 2(d) show a decrease in the electric field when the QW thickness increases from 1 to 3 ML (see Supplemental Material [19] for a discussion of critical layer thickness). This is attributed to the finite thickness of the GaN in the calculations, which really represent a GaN/InN superlattice. The same effect is observed in model calculations [20] [also shown in Fig. 2(d)] based on theoretical spontaneous polarization and piezoelectric constants for bulk GaN and InN [21]. The difference between the model and the first-principles results for 1–3 ML is likely due to the fact that the strains in InN are so large as to be outside the linear regime, linearity being an assumption in the model calculations.

The additional decrease in field when the QW thickness exceeds 3 ML is due to another effect not captured in the model, namely that when the potential drop over the InN layer exceeds its band gap, charge transfer occurs from valence-band states on one side of the well to conduction-band states on the other, leading to screening of the polarization field. The onset of this effect coincides with the point where the energy gap of the overall system goes to zero [Fig. 2(c)].

In order to further examine whether our proposed structure can undergo a topological quantum phase transition, we constructed a six-band effective model Hamiltonian based on the eight-band $\mathbf{k} \cdot \mathbf{p}$ model (Kane model) for wurtzite semiconductors. Distinct from the HgTe system [4], however, the HH and LH states in the InN system are close in energy. Therefore, a six-band effective low-energy Hamiltonian is used here, expressed by the basis $|E, \uparrow\rangle$, $|LH, \uparrow\rangle$, $|HH, \uparrow\rangle$, $|E, \downarrow\rangle$, $|LH, \downarrow\rangle$, $|HH, \downarrow\rangle$; its exact form is described in the Supplemental Material [19].

The $\mathbf{k} \cdot \mathbf{p}$ simulations show that the band structure of the GaN/InN/GaN QW is inverted when the QW width is larger than 15.5 Å [Fig. 3(a)]. This thickness, corresponding to about 5 InN layers, is somewhat larger than that of 3 to 4 InN MLs obtained in the first-principles calculations [19]. However, this difference does not affect the key features of the TI transition. The $\mathbf{k} \cdot \mathbf{p}$ model enables us to discuss the interplay of several important factors such as strain, polarization and spin-orbit interaction and to reveal the underlying physics of the TI transition. It allows us to to demonstrate the presence of edge states in a spin Hall bar, which is a direct way of identifying the TI phase. There is always an odd number of Kramers pairs of edge states on the boundary of a topological insulator [1,2]. The edge-state energy spectrum can be obtained by solving the effective six-band model for a Hall bar structure with a finite width.

To illustrate the TI state for a GaN/InN/GaN QW, we calculated the edge states of a Hall bar constructed perpendicular to the growth plane [Fig. 3(b)]. The resulting band structure is presented in Fig. 3(c) together with the density distribution of a Kramers pair of edge states. The presence of edge states in the gap between the E1 and LH1 subbands is clearly demonstrated, and the distribution of these states in real space shows that they are highly localized in the vicinity of the edges of the Hall bar. These edge states are topologically invariant under scattering, and therefore the corresponding mean free paths of the carriers can be exceedingly large. We note that although the HH band has only a slight effect on the formation of the TI state, its inclusion is important when considering the experimental detection of edge states. Like in other TI systems [22], the HH band in a quantum spin Hall bar can create flat subbands and conceal the topological edge states. However, the edge states can still be observed in the minigap between the E1 and HH1 bands [see Fig. 3(c)]. This minigap is found to be 10 meV in our system. While small, this is larger than the hybridized minigap in the InAs/GaSb QW system in which edge states have recently been observed [22].

Spin-orbit interaction is essential in the transition to a TI state. The intrinsic SOI in both InN and GaN is very small, on the order of a few meV. However, in the vicinity of an

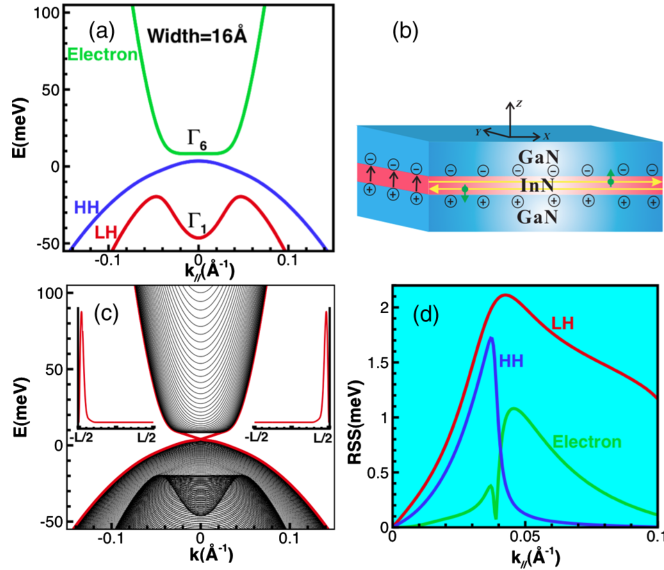

FIG. 3 (color online). (a) Band structure of a 16 Å GaN/InN/GaN QW obtained from the six-band effective Hamiltonian. (b) Schematic of an infinite long spin Hall bar with a width (along y) of 1000 Å. The thickness along the [0001] growth direction (labeled as z) comprises the InN QW plus two 200-Å-thick GaN barrier layers on either side. The yellow lines show the helical edge states, and the green arrows show the spin orientation. The short black arrows indicate the polarization-induced electric field. (c) Band structure of the Hall bar obtained by solving the effective six-band model. The insets show the density distributions of one Kramers pair of edge states: on the left the spin-up state at $k_{\parallel} = -0.1$ Å^{-1}, on the right the spin-down state at $k_{\parallel} = 0.1$ Å^{-1}. (d) Rashba spin splitting (RSS) of electron (green), HH (blue) and LH (red) subbands.

inverted-band transition, a small SOI is sufficient to drive the TI transition. Furthermore, we found that the large polarization field induces a considerable Rashba SOI. The Rashba SOI in QWs has attracted attention because it can be adjusted by gate voltage [23,24] and band engineering [25,26]. It thus provides a controllable approach to enhancing spin-polarized transport in nonmagnetic semiconductors. From the eight-band Kane model, we estimate the strength of this Rashba SOI to be on the order of 1 to 2 meV [Fig. 3(d)]. This is comparable to the Rashba SOI induced by an external electric field in InAs and HgTe quantum wells [11,12]. A Rashba SOI of this magnitude usually occurs only in systems containing heavier atoms. The unusually large Rashba SOI in GaN/InN/GaN QWs is due to the strength of the polarization field, which easily exceeds 10 times the strength of an applied electric field resulting from a gate voltage. Such a large Rashba effect was noted in a previous study on a GaN/$In_{0.5}Ga_{0.5}N$/GaN QW [27].

The proposed inverted band semiconductor structure based on thin InN QWs and the presence of a TI state offer considerable advantages over other systems including graphene [3], the Bi chalcogenides [7], and the Heusler compounds [8]. GaN/InN/GaN QW structures can be integrated in nitride-based transistors, which are already extensively used in high-frequency and high-power devices [28]. Because charge carriers can screen the polarization fields, the polarization potential can be controlled by adjusting the carriers densities in the QW, and therefore the TI transition can be controlled by doping or applying a bias voltage.

High quality InN layers in GaN matrix with a thickness of 1–2 ML and atomically sharp interfaces have already been fabricated [29,30]. Both photoluminescence [29] and electroluminescence [31] originating from electron-hole recombination have been observed. We have estimated that the critical thickness of InN layers pseudomorphically grown on a GaN substrate is as large as 17 Å, which corresponds to more than 5 InN MLs [19]. This is sufficient to allow the topological insulator transition to occur.

In summary, based on first-principles calculations and an effective low-energy $\mathbf{k} \cdot \mathbf{p}$ model, we have demonstrated that ultrathin GaN/InN/GaN QWs can undergo an inverted band transition and become a topological insulator. This quantum phase transition is driven by the strong polarization fields originating from the wurtzite symmetry and lattice mismatch, and by the Rashba spin-orbit interaction resulting from the field. This is the first demonstration of the formation of a TI phase caused by intrinsic polarization in commonly used semiconductors with weak intrinsic SOI. Since polarization fields occur in many materials, a similar mechanism may apply to other systems as well. Our approach may pave the way toward integrating controllable TIs with conventional semiconductor devices.

We thank Professor X.-L. Qi for valuable discussions. M. S. M. was supported as part of the Center for Energy Efficient Materials, an Energy Frontier Research Center funded by the U.S. DOE-BES (Grant No. DE-SC0001009). M. S. M. also thanks the ConvEne-IGERT Program (NSF-DGE0801627) and the MRSEC program (NSF-DMR1121053). Q. Y. was supported by the UCSB Solid State Lighting and Energy Center. C. V. d W. was supported by NSF under Grant No. DMR-0906805. W. K. L, L. L. L. and K. C. were supported by the National Basic Research Program of China (973 Program) under Grant No. 2011CB922204 and the NSF of China under Grant No. 10934007. The electronic structure calculations made use of NSF-funded TeraGrid resources under Grant No. DMR07-0072N.

*miaoms@engineering.ucsb.edu
†kchang@semi.ac.cn

[1] M. Z. Hasan and C. L. Kane, Rev. Mod. Phys. **82**, 3045 (2010).
[2] X. L. Qi and S. C. Zhang, Rev. Mod. Phys. **83**, 1057 (2011).

[3] C. L. Kane and E. J. Mele, Phys. Rev. Lett. **95**, 226801 (2005).

[4] B. A. Bernevig, T. L. Hughes, and S. C. Zhang, Science **314**, 1757 (2006).

[5] M. Konig, S. Wiedmann, C. Bruene, A. Roth, H. Buhmann, L. W. Molenkamp, X. L. Qi, and S. C. Zhang, Science **318**, 766 (2007).

[6] H. J. Zhang, C. X. Liu, X. L. Qi, X. Dai, Z. Fang, and S. C. Zhang, Nat. Phys. **5**, 438 (2009).

[7] D. Hsieh, D. Qian, L. Wray, Y. Xia, Y. S. Hor, R. J. Cava, and M. Z. Hasan, Nature (London) **452**, 970 (2008).

[8] S. Chadov, X. L. Qi, J. Kubler, G. H. Fecher, C. Felser, and S. C. Zhang, Nature Mater. **9**, 541 (2010).

[9] H. Lin, L. A. Wray, Y. Q. Xia, S. Y. Xu, S. A. Jia, R. J. Cava, A. Bansil, and M. Z. Hasan, Nature Mater. **9**, 546 (2010).

[10] M. Franz, Nature Mater. **9**, 536 (2010).

[11] W. Yang, K. Chang, and S. C. Zhang, Phys. Rev. Lett. **100**, 056602 (2008).

[12] J. Li and K. Chang, Appl. Phys. Lett. **95**, 222110 (2009).

[13] J. Wu, W. Walukiewicz, K. M. Yu, J. W. Ager, III, E. E. Haller, Hai Lu, W. J. Schaff, Y. Saito, and Y. Nanishi, Appl. Phys. Lett. **80**, 3967 (2002).

[14] P. Rinke, M. Winkelnkemper, A. Qteish, D. Bimberg, J. Neugebauer, and M. Scheffler, Phys. Rev. B **77**, 075202 (2008).

[15] P. E. Blöchl, Phys. Rev. B **50**, 17 953 (1994).

[16] G. Kresse and J. Furthmuller, Phys. Rev. B **54**, 11 169 (1996).

[17] J. Heyd, G. E. Scuseria, and M. Ernzerhof, J. Chem. Phys. **118**, 8207 (2003); **124**, 219906 (2006).

[18] P. G. Moses and C. G. Van de Walle, Appl. Phys. Lett. **96**, 021908 (2010).

[19] See Supplemental Material at http://link.aps.org/supplemental/10.1103/PhysRevLett.109.186803 for details of strain effects, critical layer thickness, polarization fields, and $\mathbf{k} \cdot \mathbf{p}$ Hamiltonian.

[20] V. Fiorentini, F. Bernardini, F. Della Sala, A. Di Carlo, and P. Lugli, Phys. Rev. B **60**, 8849 (1999).

[21] F. Bernardini, V. Fiorentini, and D. Vanderbilt, Phys. Rev. B **56**, R10024 (1997).

[22] I. Knez, R.-R. Du, and G. Sullivan, Phys. Rev. Lett. **107**, 136603 (2011).

[23] J. Nitta, T. Akazaki, H. Takayanagi, and T. Enoki, Phys. Rev. Lett. **78**, 1335 (1997).

[24] D. Grundler, Phys. Rev. Lett. **84**, 6074 (2000).

[25] R. Winkler, *Spin-Orbit Coupling Effects in Two-Dimensional Electron and Hole Systems* (Springer-Verlag, Berlin, 2003).

[26] W. Zawadzki and P. Pfeffer, Semicond. Sci. Technol. **19**, R1 (2004).

[27] V. I. Litvinov, Appl. Phys. Lett. **89**, 222108 (2006).

[28] U. K. Mishra, L. Shen, T. E. Kazior, and Y. F. Wu, Proc. IEEE **96**, 287 (2008).

[29] A. Yoshikawa, S. B. Che, W. Yamaguchi, H. Saito, X. Q. Wang, Y. Ishitani, and E. S. Hwang, Appl. Phys. Lett. **90**, 073101 (2007).

[30] S. Che, A. Yuki, H. Watanabe, Y. Ishitani, and A. Yoshikawa, Appl. Phys. Express **2**, 021001 (2009).

[31] E. Dimakis, A. Y. Nikiforov, C. Thomidis, L. Zhou, D. J. Smith, J. Abell, C.-K. Kao, and T. D. Moustakas, Phys. Status Solidi A **205**, 1070 (2008).